Computer-aided study of the impedance dispersion of biological tissues

Computer-aided study of the impedance dispersion of biological tissues

V N Malikov[1], N D Tihonsky[1], V N Kozlova[1], A V Ishkov[2]

[1]Altai State University, 61 Lenina ave., Barnaul, 654049, Russia
[2]Altai State Agricultural University, 98 Krasnoarmeisky ave., Barnaul, 654049, Russia

E-mail: osys11@gmail.com

Abstract. The article considers the development of a software and hardware system to study the impedance dispersion of biological fluids and tissues using an alternating signal generated and received by SensorDaq and LabView software. The design and development of the impedance measurement software and hardware system are described in detail. The impedance and capacitance values of the biological object were obtained when scanning at various frequencies and temperatures corresponding to different object conditions. The results of the system testing are shown, and the conclusions on the interaction nature of biological tissue and an external current are drawn.

1. Introduction

The need to monitor tissue composition is persistent for many applications. Bioimpedance analysis (BIA), which is the measurement of the ability of the tissue to resist electrical current as a function of frequency, provides a non-invasive method to monitor tissue properties effectively [1]. BIA has a long history in healthcare [2].

Applications include nutritional assessment for body fat and water content [3, 4], physiological assessment of vascular function [5], biosensors for determining cell activity, aging, disease [6-8], flow cytometry, and lab-on-a-chip applications. [9]. Thus, bioimpedance is a powerful method for non-invasive analysis of various types of tissues and living systems. Many earlier works have looked at the history and applications of bioimpedance in health care [10], this article looks at the BIA in terms of biophysical models and equivalent circuits with an emphasis on its applications for vascular tissue and flow analysis in both human and plant systems [11, 12, 13].

Bioimpedance analysis (BIA) is an emerging noninvasive technology which uses the electrical properties of tissues to determine several physiological modalities. It is the gold standard for body fat / water composition and tissue / organ imaging, and presents itself as a candidate for noninvasive hemodynamic monitoring.

BIA is a non-invasive method of measuring the electrical impedance of the body at alternating current frequencies. This is a convenient tool that it can be easily and rapidly performed at a patient's bedside [14, 15]. Because the resistance and reactance characteristics of bioimpedance analysis are related to body composition, in terms of muscle, fat and body water content, some studies have investigated the value of it in nutritional aspect in assessment of body composition, such as fat mass or fat-free mass in various conditions, as well as volume status [15]. The principle of BIA involves passing a small single- or multiple-frequency alternating current (1-10 μA) through the body and measuring the resulting

impedance comprising resistance and capacitive reactance. The cell membrane can be considered as a capacitor when exposed to an alternating current due to its nonconductive lipid bilayer structure [16]. When the current passes, it is considered that the extracellular fluid mainly shows the resistance[R] characteristics, while the cells show the reactance [Xc] characteristics. Measured data from a low frequency as 5 kHz, at which the current cannot penetrate the cells' membranes, is considered to be associated with extracellular water (ECW); while data from a high frequency as 200 kHz, at which the current is strong enough to penetrate the cell membrane, is considered to be associated with total body water (TBW). From these rationale basis, regression equations using data of BIA measurements have been established to calculate the body's fluid composition including Q1 ECW, TBW, and intra-cellular water (ICW) and to assess the fluid status; which is, however, still awaiting further validation. Since BIA patterns including resistance, reactance, total impedance (Z) and its variation with current frequency are considered to be theoretically associated with the disease severity-reflecting factors such as fluid status, body composition and the cells' conditions [17], its potential value in prognosis prediction is worthy of investigation [18].

The BIA can provide an assessment of body regions by measuring the resistance and reactance of biological tissue at a variety of low and high frequency electrical currents. Resistance indicates the conductive characteristics of bodies and fluids and increases as the proportion of fat and bone in the tissue increases, but decreases as the proportion of water and muscle in the tissue increases. Reactance is the resistance of a capacitor to alternating current and indicates the capacity of the cell membrane, which is related to the volume of intracellular water. These two electrical values are used in calculations using general electrical property equations to generate data for regression models with approximate composition measurements.

The primary circuit for the BIA consists of the following components: a signal generator for AC fundamental currents, current electrodes for pushing current through the material, and voltage electrodes for measuring the voltage drop across the volume of interest. The specific classification of the material electrode system depends on the number and location of the electrodes. Two common types are two-electrode and four-electrode configuration [13].

The two-electrode system uses a single pair of electrodes to act both as the current and voltage electrode. It results in a compact and simple system, the measured voltage is less sensitive due to involuntary/involuntary movement during measurement and from contact impedance interference of the electrode [19]. Despite these limitations, the two-electrode system has been widely used in impedance measurement for cell culture analysis [20], the porosity of 3D scaffold [21] and monitoring the cell growth process in implants [22]. Margo, Katrib, Nadi, and Rouane [22] developed a new bioimpedance measurement chip in the four-electrode configuration. This chip was employed to reduce the errors due to interface impedance between the measured sample and electrodes [13].

The objective of the study is to design an experimental setup to study the impedance dispersion of biological fluids and tissues using modern techniques of digital signal processing.

2. Materials and methods

To study the nature of the dependence of the resistance of biological tissue on the alternating current frequency, an experimental setup that allows measuring the impedance of the biological object has been developed. The setup was designed in two versions, an analog one and using modern digital data processing tools. Digital data processing tools make it possible to represent the signal not as a continuous spectrum but as discrete bands of analog levels. The schematic circuit of the setup for measuring the impedance of the biological object is given in figure 1.

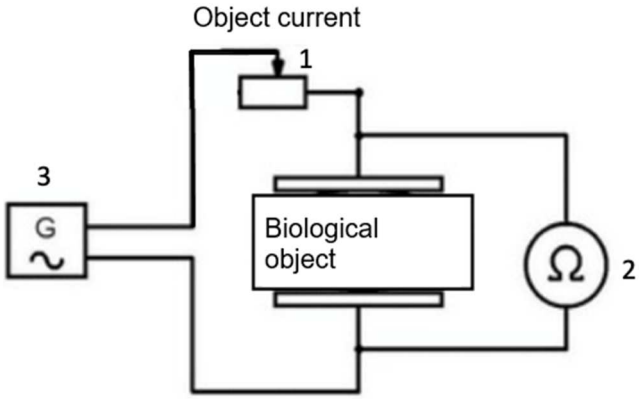

Figure 1. Test schematic circuit for measuring the impedance of the biological object.

Initially, only analog technique was used to build this circuit to test the setup performance when studying the impedance dispersion of biological tissues.

A sliding rheostat (1) was used as part of the setup. It was used to adjust the signal amplitude. The rheostat was connected to the circuit via two terminals, the lower one from the coil and the upper one where the metal rod is located. If the rheostat is connected to the circuit in this way, the current passes through the lower terminal not across the turns of the coil but along them. Then the current flows through the sliding contact along the metal rod and then returns to the circuit. Thus, only a part of the coil was used in the circuit. When we move the rheostat slider, the resistance of the part of the coil used in the circuit changes. The coil length, resistance, and current in the circuit changes as well.

Initially, an analog variable frequency oscillator (2) RSN – 18 zav No. 67 (oscillator with a frequency range from 200 kHz to 5.5 kHz) was used in the setup. The resistance value was measured by an ohmmeter (3). The disadvantage of the setup was the inability to quickly obtain the dependence of the impedance on various parameters. Thus, the setup was redesigned by adding digital elements to the electric circuit.

In the developed software and hardware system, the AFS Sensor DAQ module managed by LabVIEW software environment was used as a signal generator and receiver. Built-in digital sensors measure various parameters of the test object and display them on the screen.

In the study, the developed software and hardware system allowed accomplishing the following tasks:

1. Register the voltage variations when an alternating current penetrates biological tissue.
2. Graphically present the voltage dependencies of various parameters of the test object.
3. Determine a numerical value for voltage that carries information on the biological object parameters.

3. Experimental results

In the first experiment, a simulation of scanning biological fluid was carried out. A NaCl solution was used as the object of the study since the concentration of sodium in blood plasma corresponds to the saline solution concentration (0.9 % NaCl). The resistance of the biological object Z at different alternating current frequencies (in the range of 500 Hz – 5000 Hz) was measured at three temperatures:

t = 25 °C - room temperature.

t = 36 °C - the temperature close to normal body temperature.

t = 42 °C – the temperature at which the denaturation of muscle proteins begins.

According to the readout results of all setup sensors, the average values of the impedance Z and the standard deviations for the impedance of the biological object were found. In addition, the capacitance variation of the biological object under the influence of alternating current was recorded. The results obtained during the experiment are included in tables 1-3 and figures 2 and 3.

Table 1. Impedance dispersion of the NaCl solution at t = 25 °C.

No.	*v*, Hz	*Z*, Ohm	C, μF
1.	500	290.75	2.96
2.	1500	255.29	1.15
3.	2500	245.93	0.72
4.	3500	241.34	0.53
5.	4500	238.65	0.42
6.	5000	234.54	0.38

Table 2. Impedance dispersion of the NaCl solution at t = 36 °C.

No.	v, Hz	Z, Ohm	C, μF
1.	500	262.05	3.42
2.	1500	234.02	1.28
3.	2500	220.74	0.80
4.	3500	212.74	0.62
5.	4500	205.65	0.49
6.	5000	209.75	0.46

Table 3. Impedance dispersion of the NaCl solution at t = 42 °C.

No.	*v*, Hz	*Z*, Ohm	C, μF
1.	500	226.04	4.02
2.	1500	201.06	1.57
3.	2500	186.54	1.05
4.	3500	174.34	0.83
5.	4500	160.54	0.75
6.	5000	155.97	0.71

The obtained data was used to plot impedance-frequency graphs at various temperatures of the NaCl solution (figure 2).

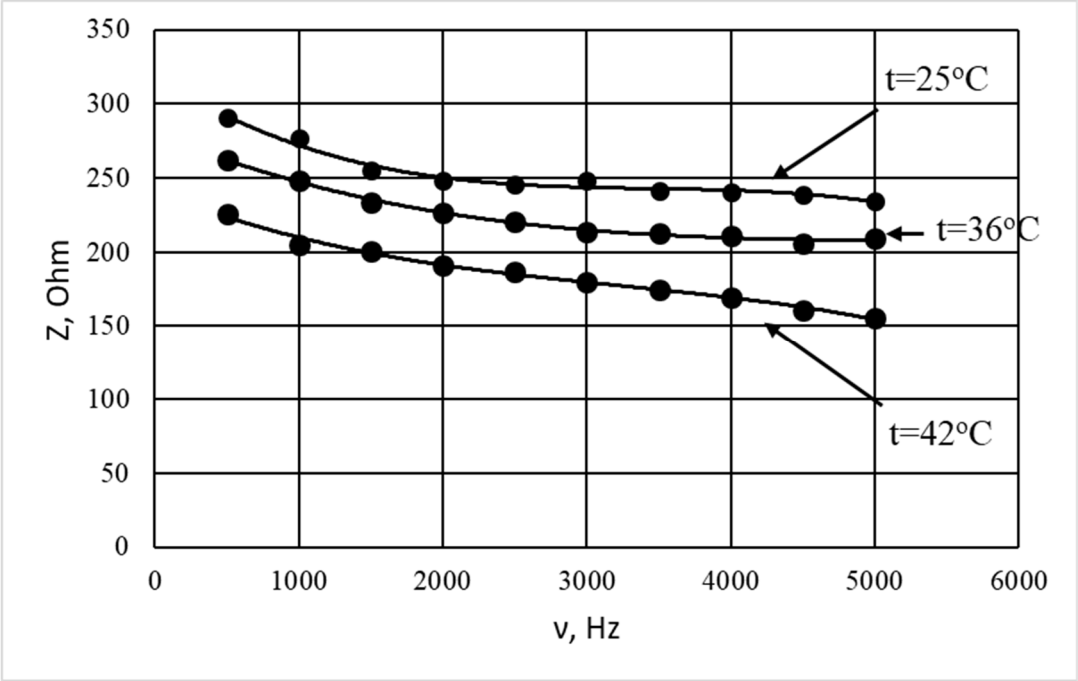

Figure 2. Variation of impedance with frequency at various temperatures of NaCl solution.

The obtained graphs were approximated by a third-order equation. The equation describing the functional relationship Z(ν) is as follows:

$$Z = -2\cdot10^{-9}\nu^3 + 2\cdot10^{-5}\nu^2 - 0.0641\nu + 319.76 \text{ at } t = 25\ ^\circ\text{C};$$
$$Z = -6\cdot10^{-10}\nu^3 + 7\cdot10^{-6}\nu^2 - 0.0352\nu + 276.93 \text{ at } t = 36\ ^\circ\text{C};$$
$$Z = -8\cdot10^{-10}\nu^3 + 8\cdot10^{-6}\nu^2 - 0.0359\nu + 239.93 \text{ at } t = 42\ ^\circ\text{C}.$$

The dependence of the sample capacitance on changes in temperature and frequency was also studied. The results of the study are shown in figure 3.

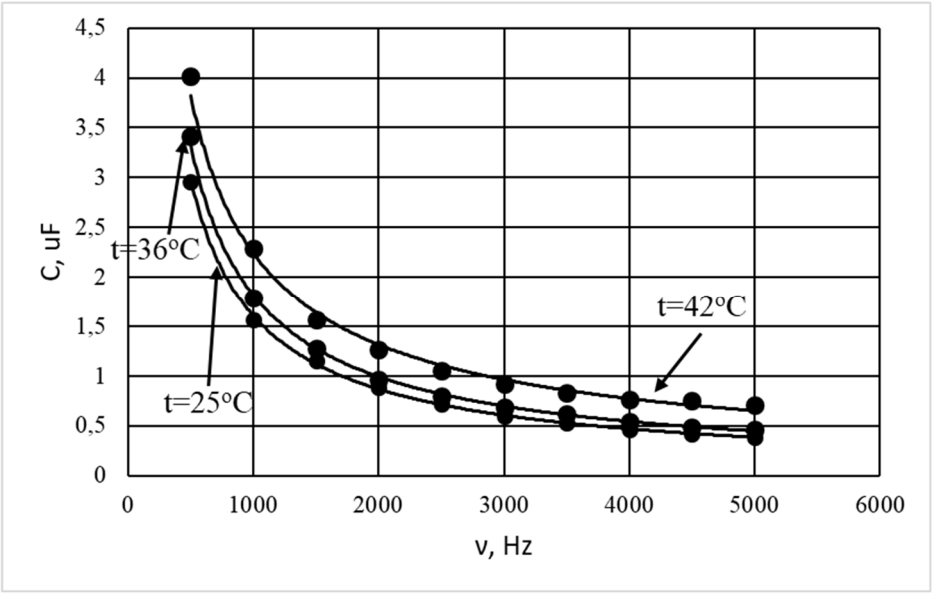

Figure 3. Variation of capacitance with frequency at various temperatures of NaCl solution.

The obtained graphs were approximated by an exponential equation. The equation describing the functional relationship C(ν) is as follows:

$$C = 756.39\nu^{-0.891} \text{ at } t = 25\ ^\circ C;$$

$$C = 753.84\nu^{-0.873} \text{ at } t = 36\ ^\circ C;$$

$$C = 454.44\nu^{-0.769} \text{at } t = 42\ ^\circ C.$$

The second experiment involved a simulation of scanning muscle tissue. The results obtained during scanning are included in tables 4-6 and figures 4 and 5.

Table 4. Impedance dispersion of biological tissue at t = 25 °C

No.	*v*, Hz	*Z*, Ohm	C, μF
1.	500	418.21	1.98
2.	1500	415.22	0.66
3.	2500	404.65	0.41
4.	3500	390.79	0.30
5.	4500	368.15	0.25
6.	5000	368.01	0.23

Table 5. Impedance dispersion of biological tissue at t = 36 °C.

No.	*v*, Hz	*Z*, Ohm	C, μF
1.	500	406.21	2.04
2.	1500	387.07	0.72
3.	2500	376.79	0.44
4.	3500	360.29	0.33
5.	4500	368.07	0.25
6.	5000	367.99	0.23

Table 6. Impedance dispersion of biological tissue at t = 42 °C.

No.	*v*, Hz	*Z*, Ohm	C, μF
1.	500	382.66	2.17
2.	1500	368.53	0.76
3.	2500	354.97	0.47
4.	3500	347.16	0.35
5.	4500	345.06	0.27
6.	5000	155.97	0.25

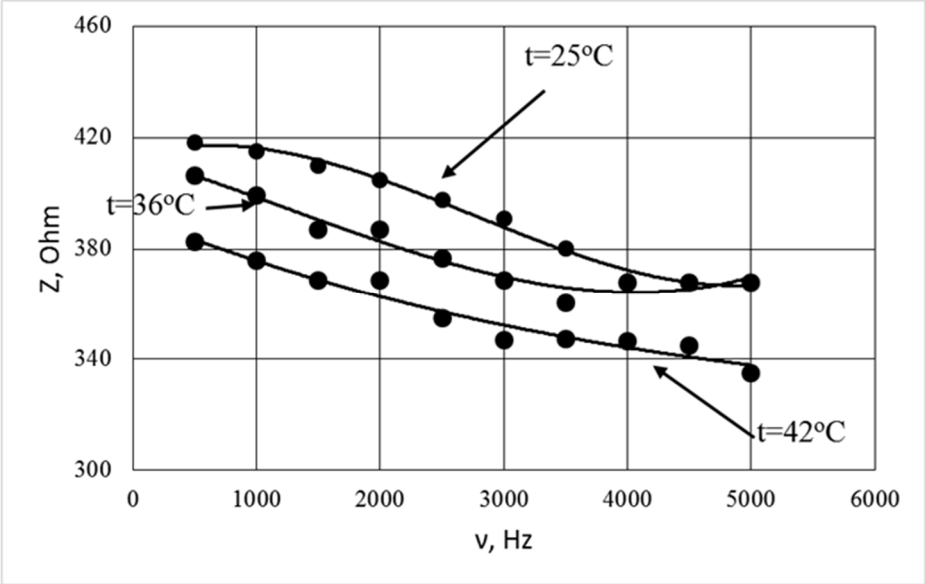

Figure 4. Variation of impedance with frequency at various temperatures of biological tissue.

The obtained graphs were approximated by a third-order equation. The equation describing the functional relationship Z(ν) is as follows:

$$Z = 7E\text{-}10\nu^3 - 8E\text{-}06\nu^2 + 0.0126\nu + 412.83 \text{ at } t = 25\ ^\circ C;$$

$$Z = 7E\text{-}10\nu^3 - 2E\text{-}06\nu^2 - 0.0132\nu + 413.51 \text{ at } t = 36\ ^\circ C;$$

$$Z = 3E\text{-}10\nu^3 - 5E\text{-}07\nu^2 - 0.0135\nu + 389.83 \text{ at } t = 42\ ^\circ C.$$

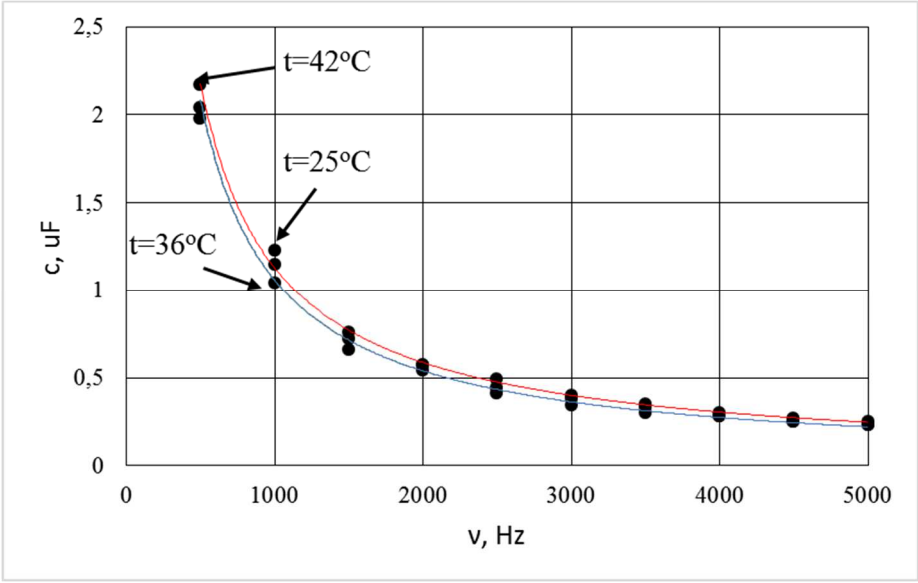

Figure 5. Variation of capacitance with frequency at various temperatures of biological tissue.

The obtained graphs were approximated by an exponential equation. The equation describing the functional relationship C(ν) is as follows:

$$C = 652.47\nu^{-0.940} \text{ at } t = 25 \text{ °C};$$

$$C = 723.99\nu^{-0.946} \text{at } t = 36 \text{ °C};$$

$$C = 736.68\nu^{-0.940} \text{at } t = 42 \text{ °C}.$$

The impedance-capacitance dispersion curve allows analyzing the state of the biological object and its abnormalities.

When the alternating field frequency increases, different structures of biological tissues are polarized. Therefore, three types of dispersion can be distinguished when studying the dependence of living tissue impedance on frequency.

At low frequencies, all structures of biological tissue (cells, large molecules of organic compounds, and water molecules) react to changes in the electric field.

The impedance dispersion in the low frequency range (alpha dispersion) is due to a decrease in the polarization effect of the surface of cells and organs surrounded by membranes. It is observed in the range from about 0.1 kHz to 1 kHz. For this section of the graph, the rate of the capacitance variation with frequency has a maximum value. In this region, the capacitance resistance of cell membranes is very high, thus electric currents that envelop the cells and flow through electrolyte solutions surrounding the cells predominate.

The second type of dispersion (beta dispersion) is observed in the frequency range from 10^3-10^8 Hz. It is due to the cytoplasmic membrane polarization, as well as the dipole polarization of large molecules of organic compounds, proteins, nucleic acids, which are stable dipoles with a large electric moment, as well as water molecules. For this section of the graph, the rate of the capacitance variation with frequency has a much lower value than that in the case of alpha dispersion.

4. Conclusion

From the above, the following conclusions can be drawn:

1. Graphs Z(v) allow studying the structure of the biological object, which determines the nature of its interaction with an external current expressed in differences in the dielectric permittivity and electrical conductivity of tissues. Cellular and intracellular membranes obstruct the free movement of ions resulting in capacitive reactance. The restricted mobility of charges around an alternating electric field leads to the polarization voltage in tissues, which triggers an increase in the reactance Z.

2. The analysis of the dispersion curves Z(v) at various object temperatures revealed that the higher the temperature, the lower the dispersion curve is located, that is, an increase in temperature causes the decrease of the impedance Z in the range of 500 Hz – 5000 Hz. This is due to the increasing rate of ion chaotic (thermal) movement in the biological object affected by the rising temperature, making the active resistance R decrease.

References

[1] Martinsen O G 2011 *Bioimpedance and bioelectricity basics* (London: Academic Press) p 547
[2] Nyboer J 1950 *Circulation* **2** 811-821
[3] Cornier M A 2011 *Circulation* **124** 1996-2019
[4] Gibson A L and Wagner D *Human Kinetics* **8** 1-8
[5] Sweitzer N K, Shenoy M and Stein J H 2007 *Diabetes Care* **36** 907–910
[6] Collins A R, Annangi B, Rubio L 2017 *Wiley Interdisciplinary Reviews: Nanomedicine and Nanobiotechnology* **9** 1-7
[7] Perez P, Huertas G and Maldonado-Jacobi A 2018 *Scientific Reports* **8** 1-11
[8] Reitinger S, Wissenwasser J, Kapferer W, Heer R and Lepperdinger G 2012 *Biosensors and Bioelectronics* **34** 63-69
[9] Chen J, Xue C, Zhao Y and Chen 2015 *International Journal of Molecular Sciences* **16** 9804-9830

[10] Khalil S F, Mohktar M S and Ibrahim F 2014 *Sensors* **14** 10895-10928.
[11] Lukaski H C 2013 *European Journal of Clinical Nutrition* **67** 2-9
[12] Macdonald J R 1992 *Annals of Biomedical Engineering* **20** 289-305
[13] Prasad A, Roy M 2020 *Biosystems Engineering* **197** 170-187
[14] Silva R D L, Pinho C P S and Rodrigues I G 2014 *Nutricion hospitalaria* **31(3)** 1278-1285.
[15] Kyle U G, Bosaeus I and De Lorenzo A D 2004 *Clinical Nutrition* **23(6**) 1430-1453.
[16] Ismael S, Savalle M and Trivin C 2014 *Critical Care* **18(2)** 49-62.
[17] Maioli M, Toso A and Leoncini M 2014 *Journal of the American College of Cardiology* **63(14)** 1387-1394.
[18] Yao J, Zhou M, and Xu B 2020 *Clinical Nutrition* **39 (9)** 2848-2855
[19] Webster J G 2009 *Medical instrumentation: Application and design* (John Wiley & Sons) p 339
[20] Serrano J A, Huertas G and Maldonado-Jacobi A 2018 *Sensors* **18**
[21] Canali C, Mohanty S and Emneus J 2015 *Electroanalysis* **27** 193-199
[22] Huang H H, Pan S J and Lu F H 2005 *Scripta Materialia* **53** 1037-1042
[23] Margo C, Katrib J, Nadi M and Rouane A 2013 *IEEE faible tension faible consommation* 1-4